  Bull. Chem. Soc. Jpn., 61, 2721—2726 (1988)

Surface Properties of Microcrystalline Hydrous Titanium Oxide as Obtained by Thermal Hydrolysis from a $TiCl_4$ Solution

Kenta Ooi,* Yoshitaka Miyai, Shunsaku Katoh, and Kazuhiko Sugasaka
Government Industrial Research Institute, Shikoku, 2-3-3 Hananomiya-cho, Takamatsu-shi 761
(Received January 20, 1988)

The surface properties of hydrous titanium oxides (HTiO's), as obtained by refluxing $TiCl_4$ or urea-containing $TiCl_4$ solutions at 373 K, were examined by means of nitrogen adsorption/desorption at 77 K and of fluoride ion adsorption. Their crystal phases and particle shapes were investigated by X-ray diffraction analyses and electronmicroscopic observations, respectively. The HTiO obtained from a 0.03 or 0.1 mol·dm^{-3} $TiCl_4$ solution was of an anatase type, consisting of small (about 10 nm) particles. They had pores that were 2 nm in radius, with an narrow size distribution. The HTiO obtained from a 1.0 mol·dm^{-3} $TiCl_4$ solution was of a rutile type, consisting of acicular particles. It had pores that were greater than 2 nm in radius, with a broad size distribution. All of the HTiO's obtained from ($TiCl_4$+urea) solutions were anatase types. The most probable pore radius increased from 1.9 to 3.6 nm with the increase in the initial $TiCl_4$ concentration from 0.03 to 1.0 mol·dm^{-3}. The surface properties of the anatase-type HTiO's were discussed based on the sizes and shapes of the primary crystallites and on their spatial distribution.

The adsorptive or catalytic activity of HTiO depends strongly on its surface properties. These surface properties themselves vary depending on the preparation method and conditions. There have been many studies of the surface properties of the HTiO's obtained through different methods of preparation.[1-20]

The thermal hydrolysis of titanium(IV) salt in solution is one of the most common methods for the preparation of HTiO. However, the physical properties of the HTiO precipitated vary widely, depending on the starting titanium(IV) salt compound and on the precipitation conditions.[14] Moreover, the addition of a water-soluble material during precipitation results in HTiO's with different physicochemical properties.[5] The addition of HCl helps to make a stabilized rutile structure, while the addition of sulfate ions accelerates anatase formation. The anatase formation can be explained by the fact that the formation of sulfate complexes ($Ti(OH)_3HSO_4$, $Ti(OH)_2HSO_4^+$) prefers the growth of a monofunctional complex of anatase.[16] Aqueous dispersions of monodispersed titanium dioxide spheres with modal diameters of 1 to 4 μm have been obtained by the thermal hydrolysis of highly acidic solutions of $TiCl_4$ in the presence of sulfate ions.[17] A method involving the addition of urea has also been tried[18] by analogy with the homogeneous precipitation method. The added urea stabilizes the anatase structure and depresses any change in the pore structure during heat aging.[19]

The HTiO's with high surface areas can be classified into two types in terms of their crystal phases: the amorphous and micro-crystalline types. The former is X-ray amorphous and can be thought to have a structure of a three-dimensional network of $-\overset{|}{\underset{|}{Ti}}-O-\overset{|}{\underset{|}{Ti}}-$ chains.[3] Therefore, its pore structure may depend on the degree of closslinking of the $-\overset{|}{\underset{|}{Ti}}-O-\overset{|}{\underset{|}{Ti}}-$ chains. The latter type has an X-ray diffraction pattern of anatase, rutile, or brookite, with a character of broad diffraction peaks. Since they are aggregates consisting of extremely small crystallites, their pore structures are controlled both by the size and shape of the primary crystallites and by their spatial distribution.[21]

In the present study, we investigated the surface properties of the HTiO's obtained through the thermal hydrolysis method. The effects of the initial concentration of $TiCl_4$ and of the addition of urea during thermal hydrolysis on the surface properties of HTiO were studied. The surface properties were examined by means of nitrogen adsorption/desorption at 77 K and of fluoride ion adsorption. Since the HTiO's obtained by this method are usually microcrystalline anatase or rutile, the difference in the pore structures was discussed based on a packing model for small spheres.

Experimental

Preparation of HTiO. A $TiCl_4$ solution of 0.03, 0.1, 0.3, or 1.0 mol·dm^{-3}, prepared by diluting a stock solution of 3.0 mol·dm^{-3} $TiCl_4$, was refluxed with vigorous stirring at 373 K. After 7 hours of reflux, a white precipitate which had thus been precipitated was left standing for 10 hours at room temperature, washed with water, air-dried, crushed, and sieved to a 200—300 mesh size. The products were named H-0.03, H-0.1, etc. so that the numbers corresponded to the starting $TiCl_4$ concentrations.

The concentration of the titanium(IV) ions in the reacting solution was determined by atomic absorption spectrometry in order to determine a given fraction of precipitated HTiO.

In the case of urea addition, HTiO's were prepared by the same procedure using solutions of urea-containing $TiCl_4$. The molar concentrations of urea were adjusted to twice those of $TiCl_4$. The products were named N-0.03, N-0.1, etc. as above.

The water, urea, and chloride-ion contents of the products were measured as has previously been reported.[19,20]

X-Ray Diffraction Analysis and Electronmicroscopic Observation. X-Ray diffraction analyses were made on a Rigaku-Denki D3F X-ray diffractometer using Cu $K\alpha$ radia-

tion. Transmission electronmicroscopic observations were carried out by use of a Hitachi H-800 electron microscope at 200 kV.

Nitrogen Adsorption/Desorption Isotherm. Nitrogen adsorption/desorption isotherms were obtained on a Carlo Erba 1800 Sorptomatic apparatus with samples outgassed for 4 hours below 10^{-3} mmHg (1 mmHg≈133.322 Pa) at 333 K. V_l-t plots were made from adsorption isotherms using de Boer's t-values (Al_2O_3 standard).[22] The pore-size distribution curves were calculated from the desorption branches using the method of Mikhail et al., assuming cylindrical pores.[23]

Fluoride Ion Adsorption. The amounts of the surface hydroxyl group were determined by means of fluoride ion adsorption from a acetic acid-sodium acetate buffer solution (pH 4.6)[24] using a fluoride ion-selective electrode.

Results and Discussion

Bulk Properties. The rate of HTiO precipitation was fast and was independent of the starting $TiCl_4$ concentration and of the urea concentration. More than 90% of the titanium(IV) ions were precipitated by heating for 1 hour.

The urea and chloride ion contents were less than 0.1% for all of the HTiO's. The water contents are given in Tables 1 and 2. The crystal phases varied from anatase (H-0.03, H-0.1), mixture of anatase and rutile (H-0.3), to rutile (H-1) with the increase in the initial $TiCl_4$ concentration in the case of $TiCl_4$ solutions (Fig. 1). The H-0.03 and H-1 samples correspond to the microcrystalline anatase and rutile, respectively, reported in a previous paper.[21] A previous paper showed a conversion of anatase phase into rutile during heat-aging at 353 K in the case of a 1.0 mol·dm^{-3} $TiCl_4$ solution.[19] The conversion proceeds by means of a dissolution/recrystallization mechanism. The concentrations of free titanium(IV) ions in

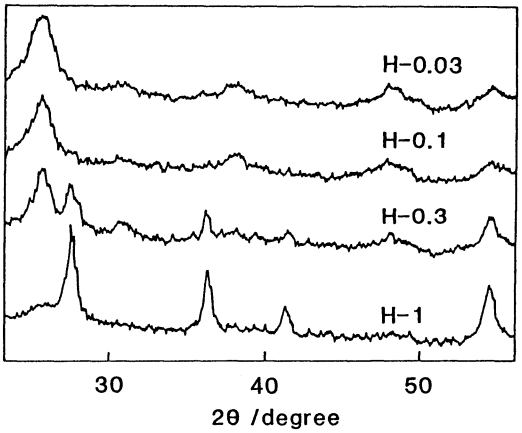

Fig. 1. X-Ray diffraction patterns of the HTiO's obtained from $TiCl_4$ solutions. Initial $TiCl_4$ concentration; H-1: 1.0 mol dm^{-3}, H-0.3: 0.3 mol dm^{-3}, H-0.1: 0.1 mol dm^{-3}, H-0.03: 0.03 mol dm^{-3}.

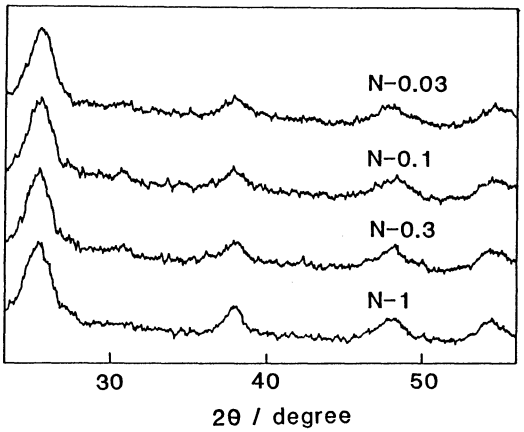

Fig. 2. X-Ray diffraction patterns of the HTiO's obtained from urea-containing $TiCl_4$ solutions. Initial $TiCl_4$ concentration; N-1: 1.0 mol dm^{-3}, N-0.3: 0.3 mol dm^{-3}, N-0.1: 0.1 mol dm^{-3}, N-0.03: 0.03 mol dm^{-3}.

Table 1. Properties of HTiO's Obtained from $TiCl_4$ Solutions

Sample	Water content	D_c	S_{BET}	S_t	V_p	N_{OH}	D_{OH}
	%	nm	$m^2 \cdot g^{-1}$	$m^2 \cdot g^{-1}$	$cm^3 \cdot g^{-1}$	$mmol \cdot g^{-1}$	nm^{-2}
H-0.03	17.4	5.5[a]	212	204	0.170	1.43	4.0
H-0.1	15.9	5.3[a]	211	200	0.195	1.38	3.9
H-0.3	13.1	9.4[b]	146	143	0.155	1.02	4.2
H-1	10.6	11.0[b]	116	108	0.244	0.87	4.5

D_c: Crystallite size estimated from X-ray diffraction pattern, a); anatase (101), b); rutile (101), S_{BET}: BET surface area, S_t: surface area obtained from V_l-t plot, V_p: pore volume, N_{OH}: amount of surface hydroxyl group, D_{OH}: surface density of hydroxyl group=N_{OH}/S_{BET}.

Table 2. Properties of HTiO's Obtained from ($TiCl_4$+Urea) Solutions

Sample	Water content	D_c	S_{BET}	S_t	V_p	N_{OH}	D_{OH}
	%	nm	$m^2 \cdot g^{-1}$	$m^2 \cdot g^{-1}$	$cm^3 \cdot g^{-1}$	$mmol \cdot g^{-1}$	nm^{-2}
N-0.03	16.8	5.3[a]	209	214	0.182	1.36	3.9
N-0.1	17.3	5.3[a]	210	208	0.201	1.38	3.9
N-0.3	15.5	5.2[a]	229	223	0.263	1.41	3.7
N-1	13.2	5.0[a]	256	240	0.382	1.41	3.4

Symbols are the same as those in Table 1.

the mother solutions were measured in the present case, after a 3-hour reflux, as 1.9, 2.0, 10, and 13 mmol·dm^{-3} at the $TiCl_4$ concentrations of 0.03, 0.1, 0.3, and 1 mol·dm^{-3}, respectively. A comparison of the solubility data with the crystal phases of the HTiO's suggests that the conversion takes place at a $TiCl_4$ concentration above 0.3 mol·dm^{-3}, while only a reinforcement of the primary particles is dominant below 0.1 mol·dm^{-3}. The crystallite sizes calculated using the Scherrer equation[25] were about 5 nm for the anatase-type HTiO's (Table 1). In the case of the ($TiCl_4$+urea) solutions, all of the HTiO's showed the X-ray diffraction patterns corresponding to that of anatase (Fig. 2).

Electronmicrographs showed that the rutile type was an aggregate of acicular particles, while the anatase types were aggregates of extremely small, nearly spherical particles (Figs. 3a and 3b). The shapes of the particles differed slightly between N-1 and N-0.03; the particles were less spherical, and their boundaries were less clear for N-1. H-0.3 was a mixture of irregular-shaped particles about 100 nm in size and spherical particles about 10 nm in size.

Surface Properties of HTiO's Obtained from $TiCl_4$ Solutions. The nitrogen adsorption/desorption isotherms were classified as being the BDDT IV type for all of the samples (Fig. 4); this is a characteristic of mesoporous materials.[26] Hysteresis loops existed at a relative pressure of around either 0.5 or 0.9; this cor-

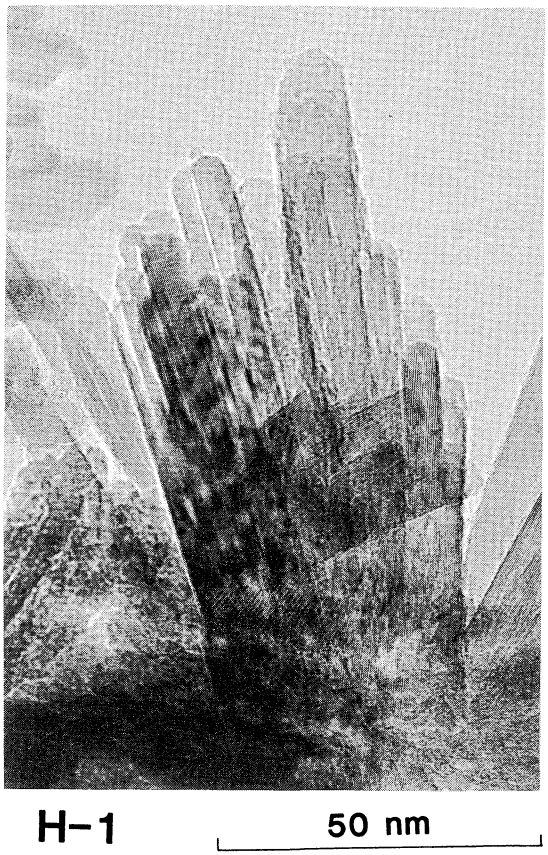

Fig. 3a. Electronmicrograph of H-1.

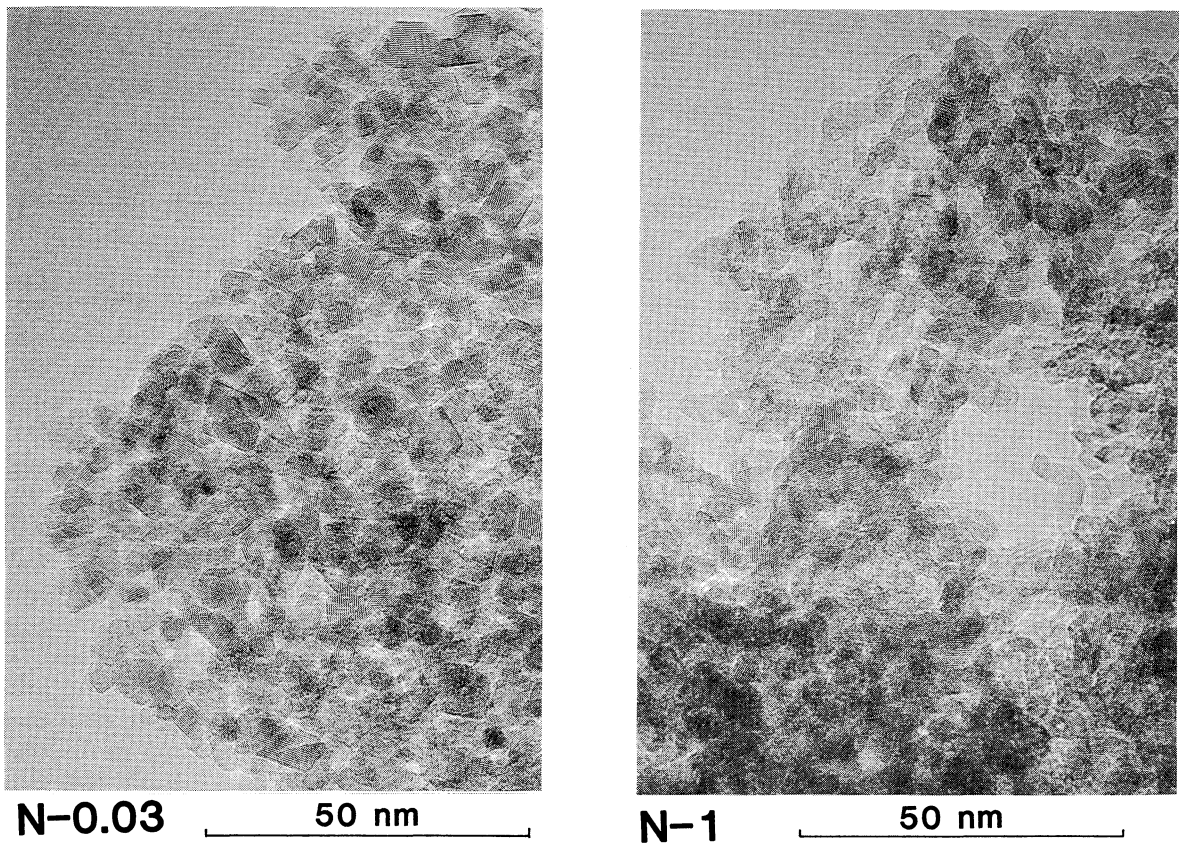

Fig. 3b. Electronmicrographs of N-1 and N-0.03.

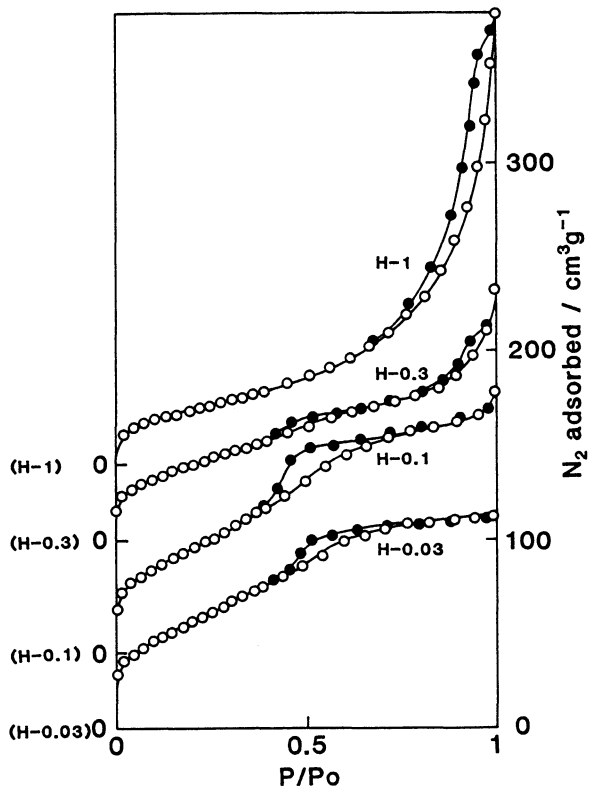

Fig. 4. Nitrogen adsorption/desorption isotherms. ○: adsorption, ●: desorption.

responds to the presence of two types of pores in these HTiO's. The BET surface area showed a tendency to decrease with an increase in the initial $TiCl_4$ concentration, probably because of the increase in the crystallite size. The V_l-t plots for H-1 and H-0.1 showed upward deviations from straight lines at $t>0.65$ and $t>0.54$ nm, respectively, due to the capillary condensation of nitrogen in the mesopores (Fig. 5). At a still higher value of t, the slope of the plot for H-0.1 tended to decrease because of the filling of the pores with liquid nitrogen. The V_l-t plots for H-0.03 and H-0.3 showed downward deviations at $t>0.57$ nm due to pore filling of nitrogen. The surface areas calculated from the slopes of the straight lines (St) agreed well with the corresponding BET surface areas (Table 1). The pore-volume distribution curves showed the presence of two types of pores: pores of a 2-nm radius with a narrow size distribution and pores with radii greater than 2 nm with a broad size distribution (Fig. 6). The former were found for the anatase-type HTiO's, and the latter, for the rutile-type HTiO. The difference in the crystal phase of the product may be responsible for the variation in pore structure in the case of $TiCl_4$ solution. The broad size distribution of the pores in the rutile-type HTiO may be caused by an irregular orientation of the rod-like particles in an aggregate.

The amounts of the surface hydroxyl group (N_{OH}) are given in Table 1. The surface densities of the hydroxyl group per unit area (D_{OH}) were calculated by using the S_{BET} values. The D_{OH} values were about 4

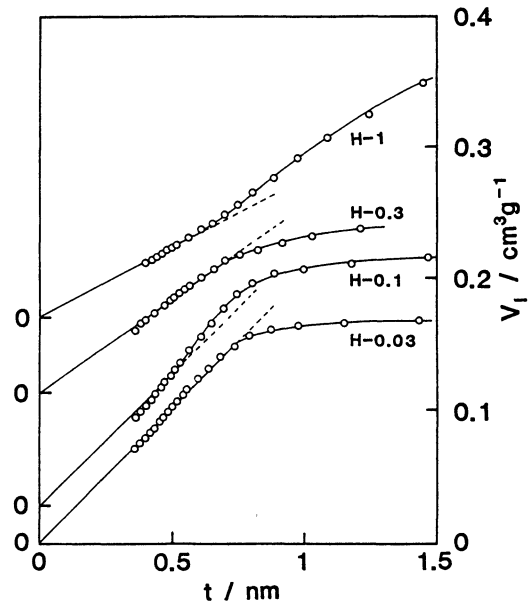

Fig. 5. V_l-t plots from nitrogen adsorption data.

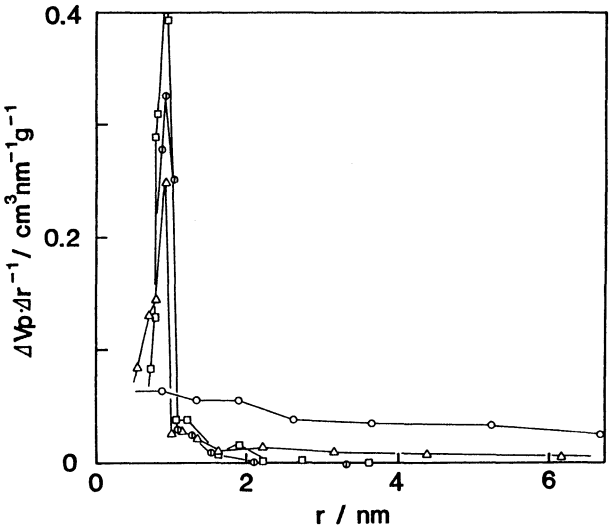

Fig. 6. Pore volume distribution curves. ○: H-1, △: H-0.3, □: H-0.01, ⊕: H-0.03.

OH/nm^2 for the anatase types, while it was slightly larger (4.5 OH/nm^2) for the rutile type (Table 1).

Surface Properties of HTiO's Obtained from ($TiCl_4$+ Urea) Solutions. The nitrogen adsorption/desorption isotherms also belonged to the BDDT IV classification for all of the HTiO's (Fig. 7). The hysteresis loop shifted to a higher relative pressure with an increase in the initial $TiCl_4$ concentration, indicating an increase in the pore size. The BET surface area increased slightly with an increase in the $TiCl_4$ concentration, while the pore volume increased markedly. The V_l-t plots showed upward deviations from straight lines at $t>0.57$ nm for N-0.1, N-0.3, and N-1 (Fig. 8). At a still higher value of t, however, the slopes of the plots for N-0.1 and N-0.3 tended to decrease. The V_l-t plot showed a downward deviation for N-

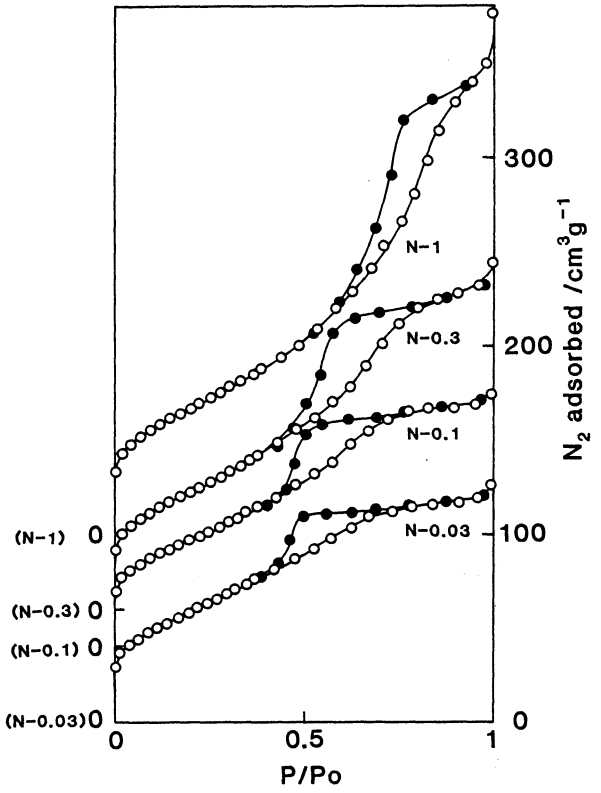

Fig. 7. Nitrogen adsorption/desorption isotherms. ○: adsorption, ●: desorption.

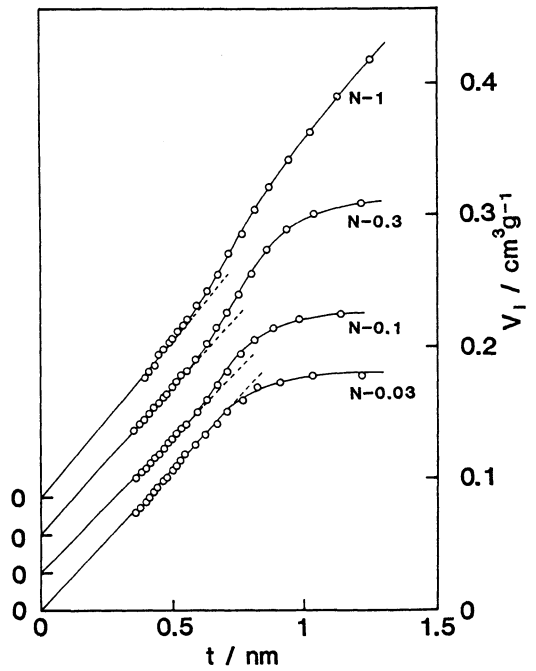

Fig. 8. V_1–t plots from nitrogen adsorption data.

0.03. The pore-volume distribution curves showed that the most probable pore radius (R_p) increased from 1.9 to 3.6 nm with an increase in the initial $TiCl_4$ concentration, accompanied by a broadening of the distribution curve (Fig. 9).

A previous study has shown that the crystal phase

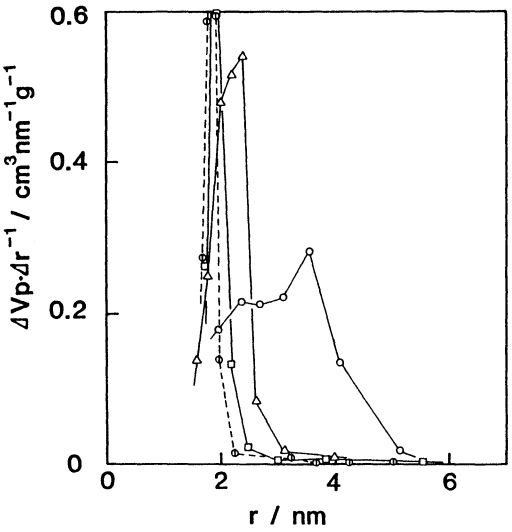

Fig. 9. Pore volume distribution curves. ○: N-1, △: N-0.3, □: N-0.1, ◇: N-0.03.

and pore structure of the precipitates are scarcely influenced by the step of heat-aging at 353 K in the case of a ($TiCl_4$+urea) solution.[19] Therefore, the pore structure is controlled mainly by the conditions during the step when the primary crystallites are precipitated and become an aggregate of a gel network. The increase in the porosity with the initial $TiCl_4$ concentration in the ($TiCl_4$+urea) system can be thought of as being due to the presence of urea at higher concentration. The addition of a water-soluble organic material before gel formation serves to provide a gel with a greater porosity.[12] Urea may play the same role.

Analysis Based on Packed-Sphere Model. The previous calculations of the surface areas of microcrystalline anatase and rutile showed that the BET surface areas correspond mainly to the external surface of the primary crystallites.[21] Therefore, their pore structures can be represented by the spatial distribution of the primary crystallites. The pore distributions of the anatase-type HTiO's could be analyzed by the use of a packed-sphere model, in which a system consisting of spherical particles of a uniform size was assumed.[27,28] According to this model, the radius of the circle (R') inscribed in the throat of the cavity among spheres can be calculated as a function of the cordination number (n) between the particles.[28] A crude estimation of the n-value can be derived from the porosity (P) of a material; this can be evaluated from the pore volume (V_p) and the particle density (ρ) as:

$$P(\%) = 100 \cdot V_p/((1/\rho) + V_p). \quad (1)$$

The porosity of the HTiO increased from 41 to 59% with an increase in the initial $TiCl_4$ concentration from 0.03 to 1 mol·dm^{-3} in the case of a urea-containing $TiCl_4$ system (the particle densities were assumed to be equal to that of anatase, ρ=3.8 g·ml^{-1})[29] (Table 3). This indicated a looser packing of the anatase crystallites with an increase in the initial

Table 3. Porosity (P), Coordination Number (n), and Pore Radius Evaluated by the Packed-Sphere Model

Sample	P	n	R'	R_p
	%		nm	nm
N-0.03	41	8	1.3	1.9
N-0.1	43	8		2.0
N-0.3	50	6		2.3
N-1	59	4—6	1.2—2.1	3.6

The packing model used was that of Avery and Ramsay.[28]
R': Radius of circle inscribed in the throat of a cavity,
R_p: most probable pore radius in Fig. 9.

$TiCl_4$ concentration. The increase in the porosity corresponded to a decrease in the cordination number (n) from 8 to about 5.

The R' values could be calculated using the averaged particle radii, which could themselves be evaluated by studying the electronmicrographs of 100 particles (3.2 nm for N-0.03 and 2.9 nm for N-1). In the case of N-0.03, the calculated R' value agreed comparatively well with the most probable pore radius (R_p), as determined by the nitrogen isotherm (Table 3). This suggested the validity of the application of the packed-sphere model to anatase-type HTiO. However, the agreement between the R_p- and R'-values was not so good in the case of N-1; the R_p value was about twice as large as the R' value. The larger R_p value in N-1 may be due to an irregular packing of the crystallites compared to the theoretical packing of primitive cubic (n=6) or tetrahedral (n=4). The irregular packing could be presumed from the broadening of the pore distribution of N-1 in Fig. 9.

The above calculations suggest the suitability of the packed-sphere model for describing the pore structure of anatase-type HTiO when the packing of the microcrystallites is relatively compact ($n>8$). In the case of a looser packing ($n<6$), however, it may be necessary to consider the diversity of the coordination number in describing an appropriate packing image of the pore structure.

The authors are grateful to Hitachi, Ltd., for its helpful support of the electronmicroscopic observation.

References

1) S. J. Gregg and M. I. Pope, *Kolloid-Z*, **174**, 27 (1961).
2) M. R. Harris and G. Whitaker, *J. Appl. Chem.*, **12**, 490 (1962).
3) M. R. Harris and G. Whitaker, *J. Appl. Chem.*, **13**, 348 (1963).
4) C. Heitner-Wirguin and A. Albu-Yaron, *J. Appl. Chem.*, **15**, 445 (1965).
5) J. P. Bonsack, *J. Colloid Interface Sci.*, **44**, 430 (1973).
6) G. D. Parfitt, K. S. W. Sing, and D. Urwin, *J. Colloid Interface Sci.*, **53**, 187 (1975).
7) A. Kurosaki and S. Okazaki, *Nippon Kagaku Kaishi*, **1976**, 1816.
8) J. Ragai, K. S. W. Sing, and R. Michail, *J. Chem. Tech. Biotech.*, **30**, 1 (1980).
9) J. Ragai and K. S. W. Sing, *J. Chem. Tech. Biotech.*, **32**, 988 (1982).
10) J. Ragai and K. S. W. Sing, *J. Colloid Interface Sci.*, **101**, 369 (1984).
11) T. M. El-Akkad, *J. Colloid Interface Sci.*, **76**, 67 (1980).
12) T. M. El-Akkad, *J. Colloid Interface Sci.*, **78**, 100 (1980).
13) M. Tsuji, M. Abe, and M. Orimo, *Bull. Chem. Soc. Jpn.*, **58**, 97 (1985).
14) K. Funaki and Y. Saeki, *Kogyo Kagaku Zasshi*, **59**, 1291 (1956).
15) K. Funaki and Y. Saeki, *Kogyo Kagaku Zasshi*, **59**, 1295 (1956).
16) E. Santacesaria, M. Tonello, G. Storti, P C. Pace, and S. Carra, *J. Colloid Interface Sci.*, **111**, 44 (1986).
17) E. Matijevic, M. Budnik, and L. Meites, *J Colloid Interface Sci.*, **61**, 302 (1977).
18) H. Suzuki, T. Iwai, T. Hasegawa, K. Okujima, C. Horie, and I. Koyama, *Nippon Kagaku Kaishi*, **1977**, 1063.
19) K. Ooi, T. Kitamura, S. Katoh, and K. Sugasaka, *Nippon Kagaku Kaishi*, **1983**, 1.
20) K. Ooi, T. Kitamura, S. Katoh, and K. Sugasaka, *Nippon Kagaku Kaishi*, **1984**, 534.
21) K. Ooi, S. Katoh, and K. Sugasaka, *J. Colloid Interface Sci.*, **119**, 595 (1987).
22) B. C. Lippens and J. H. de Boer, *J. Catal.*, **4**, 319 (1965).
23) R. Sh. Mikhail, S. Brunauer, and E. E. Bodor, *J. Colloid Interface Sci.*, **26**, 54 (1968).
24) H. P. Boehm, *Angew. Chem.*, **78**, 617 (1966).
25) H. P. Klug and L. E. Alexander, "X-ray Diffraction Procedure for Polycrystalline and Amorphous Materials," John Wiley and Sons, New York (1956), p. 491.
26) S. J. Gregg and K. S. W. Sing, "Adsorption, Surface Area, and Porosity," Academic Press, New York, (1982), p. 5.
27) D. C. Havard and R. Wilson, *J. Colloid Interface Sci.*, **57**, 276 (1976).
28) R. G. Avery and J. D. F. Ramsay, *J. Colloid Interface Sci.*, **42**, 597 (1973).
29) R. J. H. Clark, "Titanium," in "Comprehensive Inorganic Chemistry, Vol. 3," ed by J. C. Bailar, Pergamon Press, New York (1983), p. 376.